

Nitrogen-induced local magnetic and structural properties of sputtered FeAlN thin films

Y.-K. Liu^{a)} and M. H. Kryder

Data Storage Systems Center, Carnegie Mellon University, 5000 Forbes Avenue, Pittsburgh, Pennsylvania 15213-3890

D. H. Ryan and Z. Altounian

Physics Department, Centre for the Physics of Materials, Rutherford Physics Building, McGill University, 3600 University Street, Montreal QC H3A 2T8, Canada

(Presented on 12 November 2002)

Conversion electron Mössbauer spectroscopy (CEMS) and x-ray diffraction were used to study a series of rf-reactively sputtered FeAlN thin films with the goal of gaining insight into the origins of their uniaxial magnetic anisotropy (UMA) and the effect of sputtering conditions on its thermal stability. At N/Fe=4.6% ($\pm 0.5\%$), N goes into interstitial vacancies without significant reductions in the hyperfine field (B_{hf}) of the Fe but causing lattice expansions, leading to an increased linewidth in the CEMS spectra of the film while the sample has an in-plane UMA. Reducing the target-to-substrate spacing used in the deposition process does not affect the nitrogen content of the films but yields an increased CEMS linewidth reflecting larger disorder in the local Fe environment. Heavy N doping causes the phase transform into γ' -Fe₄N, ϵ -Fe₃N, and ζ -Fe₂N phases. A well defined UMA exists in mildly doped FeAlN films when doped N atoms mostly occupy the interstitial sites while FeAl and heavily doped FeAlN films are either isotropic or weakly anisotropic. UMA and its thermal stability are therefore concluded to have a correlation with the local environment of the Fe structure induced by N doping. © 2003 American Institute of Physics. [DOI: 10.1063/1.1557348]

I. INTRODUCTION

Uniaxial magnetic anisotropy (UMA) is an important property in FeXN (X=Al, Ta, etc...) thin films for magnetic recording applications. UMA in the transverse field annealing process (TFA) was reported unstable.¹ It was shown later² that reducing the target-to-substrate spacing (d_{ts}) improved the thermal stability of UMA and the unstable FeTaN films have larger Fe lattice expansions. It was suggested that the diffusion of interstitial atoms could be the cause of the thermal instability of UMA in the FeXN films² and N induced atomic arrangement could affect the diffusion barrier of the interstitial N or C in FeN or FeC materials.³ However, x-ray diffraction (XRD) spectra and x-ray photoelectron spectra could not differentiate between the films deposited at $d_{\text{ts}}=38$ mm and $d_{\text{ts}}=67$ mm.

Conversion electron Mössbauer microscopy (CEMS) was used to investigate the local structural and magnetic properties in various Fe-N materials and several iron nitride phases were identified using this method in addition to XRD analysis.^{4,5}

II. EXPERIMENTAL TECHNIQUES

A series of FeAlN films were deposited on Si(100) substrates using the rf sputtering method on a Perkin Elmer sputtering system. A 99.95% pure FeAl target with 2% *a/o* Al was used. The power density was ≈ 10 W/in.². N₂/Ar

partial pressures during the deposition processes were varied from 0% to 100%. A FeAlN film was deposited at $d_{\text{ts}}=38$ mm for comparison with the one deposited at $d_{\text{ts}}=67$ mm while other conditions were kept the same between these two samples. The background vacuum is below 5×10^{-7} Torr. A field ≈ 25 Oe was applied during the deposition process. The film thickness is 200 ± 5 nm with the exception that the FeAlN with 99.5% nitrogen to iron atomic ratio in the film (N/Fe) is 135 ± 5 nm thick. N/Fe is measured using x-ray photoelectron spectroscopy (XPS) and Rutherford backscattering spectrometry (RBS) and the error is $\pm 0.5\%$. The film thickness was determined using a Tencor profilometer and a timer linked to the target power of the sputtering system. XRD was performed using a Rigaku diffractometer and Cu $K\alpha$ line (1.54056 Å) was used for these x-ray $2\theta(\circ)$ diffraction measurements. CEMS spectra were collected using a He+10% CH₄ gas-flow proportional counter at room temperature (RT) and fitted using a nonlinear least squares fitting routine using Lorentzian lines or Lorentzian lines with a Gaussian distribution of hyperfine fields. The spectrometer was operated in constant acceleration mode and calibrated using an α -Fe foil at RT.

III. RESULTS AND DISCUSSION

N/Fe and XRD spectra of the FeAl(N) samples are shown in Fig. 1. It was found that N/Fe in the films increased from 0% to 99.5%. In the sample with N/Fe=0%, an XRD peak representing pure α -Fe was observed. In the sample with N/Fe=4.6%, it is also α -Fe but the peak position was

^{a)} Author to whom correspondence should be addressed; electronic mail: yikuang@andrew.cmu.edu

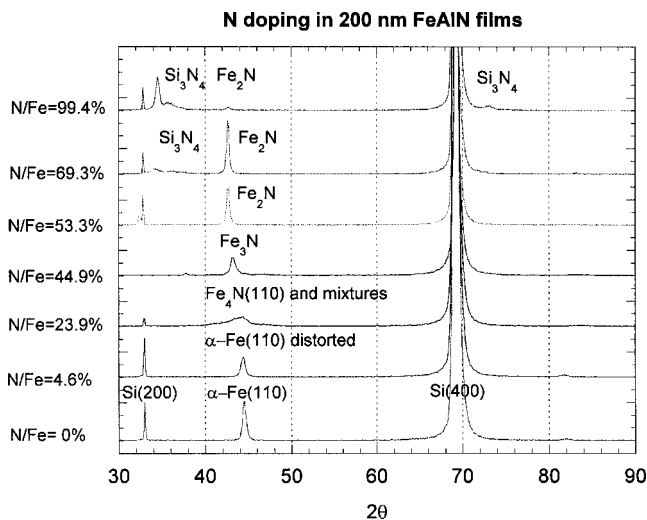


FIG. 1. XRD spectra and N/Fe of FeAlN samples with various N doping.

shifted slightly due to the lattice expansion caused by N doping. In the sample with N/Fe=23.9%, the peak is broad and hard to differentiate different phases in the films. In the sample with N/Fe=44.9%, the observed peak represents the presence of ϵ -Fe₃N. In samples with N/Fe=53.3%, 69.3%, and 99.4%, a peak represents the ζ -Fe₂N and another peak gradually appeared around $2\theta \approx 34^\circ$, a signature of Si₃N₄.

CEMS spectra of FeAlN films with N/Fe=4.6%, 23.9%, 44.9%, and 53.3% are shown in Fig. 2. CEMS spectra of the FeAl film with N/Fe=0% and the FeAlN film with N/Fe=4.0% ($d_{ts}=38$ mm) resemble one of the FeAlN films with N/Fe=4.6% ($d_{ts}=67$ mm), while the spectra of FeAlN samples with N/Fe=69.3% and 99.4% are similar to the one of N/Fe=53.3%. Major parameters used in the fitted CEMS spectra, including the area percentage [A(%)] of each component and its local magnetic and structural properties are summarized in Table I. It is noted that these CEMS area ratios do not come from direct measurements of N atoms and their contents in the films since only Fe CEMS spectra were obtained. The N/Fe ratios were accurately measured using XPS or RBS within $\pm 0.5\%$ by directly measuring the N and Fe spectra in these two measurements.

In FeAlN samples with N/Fe=0%, 4.6% ($d_{ts}=67$ mm) and 4.0% ($d_{ts}=38$ mm), the magnetic hyperfine field (B_{hf}) is around 33 T, indicating that the only phase is α -Fe. The slight deviations from $B_{hf}=33$ T in these three samples indicate that doped Al and N atoms are in the Fe local environment and cause slight reduction of B_{hf} . XRD spectra also support the observation that α -Fe is the only phase in these three films.

It is noted that the linewidth in the CEMS spectrum of the FeAlN sample deposited at $d_{ts}=38$ mm with N/Fe=4.0% is larger than the one of the FeAlN sample deposited at $d_{ts}=67$ mm with N/Fe=4.6% and the latter is larger than the one of Fe standard. A larger linewidth indicates a larger deviation from the local atomic order from the bcc α -Fe. The increase of linewidth, the reduction of B_{hf} , and the peak shift in XRD spectra from pure Fe standard to these two mildly doped FeAlN films all indicate that doped N atoms are distributed in the Fe local environment and change slightly the

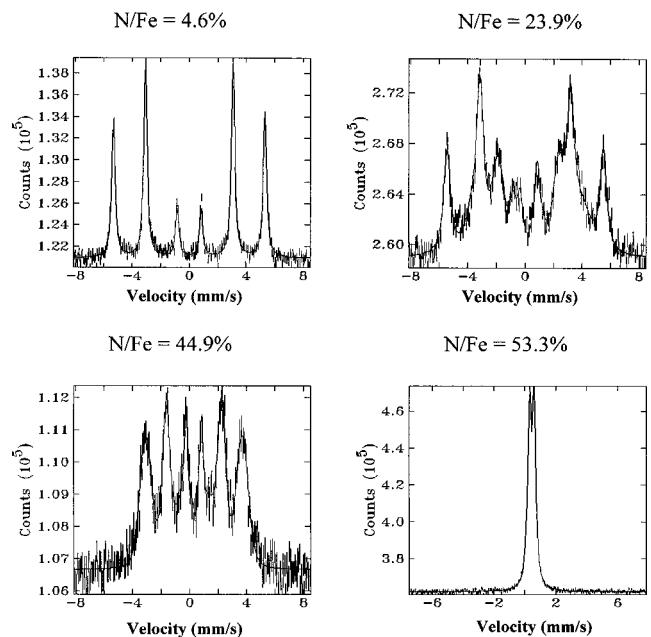


FIG. 2. CEMS spectra of FeAlN samples with N/Fe=4.6%, 23.9%, 44.9%, and 53.3%. The vertical lines represent the data point with error bars and the curves with solid lines represent the best-fitted results using the major parameters and components listed in Table I. It is noted that the sample with N/Fe=53.3% is clearly nonmagnetic. The fitting was done using the quadrupole splitting in order to estimate the isomer shift.

atomic order of the Fe lattice. It is noted that the linewidth of the FeAl film (N/Fe=0%) is comparable to that of the FeAlN film with N/Fe=4.6%, indicating that the doped Al could also disrupt the Fe local environment. However, the fitting of CEMS data of the FeAl film could not be optimized due to some background component. Therefore, it is inconclusive whether this sample could be used for comparing subtle differences. In other samples, the fitting was optimized.

The larger CEMS linewidth of the FeAlN film deposited at $d_{ts}=38$ mm with N/Fe=4.0%, compared with the one of the FeAlN film deposited at $d_{ts}=67$ mm with N/Fe=4.6%, could be caused by either some damage of the Fe lattice or a different N distribution in the Fe local environment. N/Fe did not differ greatly between these two samples. It was reported that reduced d_{ts} of 38 mm from 67 mm improved the thermal stability of UMA in TFA.² The correlation between the larger CEMS linewidth and the better thermal stability of UMA is suggested to be due to the higher energy barrier for the diffusion of N. The larger local atomic disorder could impede the diffusion of N. A much larger lattice expansion is suggested to cause a much lower energy barrier in FeTaN.^{1,2}

CEMS spectrum of the FeAlN film with N/Fe=23.9% shows that there are three major Fe-N configurations present in the film. The one with $B_{hf} \approx 34$ T corresponds to the corner Fe in the γ' -Fe₄N bcc unit cell. The one with $B_{hf} \approx 23$ T could correspond to face center Fe in γ' -Fe₄N and/or the Fe site in ϵ -Fe₃N. In addition, a small amount of the amorphous component⁴ existed. These Fe sites are better distinguished from CEMS spectrum than XRD spectrum. The relative ratio and other properties are listed in Table I. It is suggested that some excess N atoms are present around the γ' -Fe₄N and

TABLE I. Major best-fitted parameters in CEMS spectra of FeAlN samples and a Fe standard. The isomer shift is relative to α -Fe at RT.

Sample	N/Fe (%) ($\pm 0.5\%$)	R	Identified component	$B_{\text{hf}}(\text{T})$	Linewidth (mm/s) (Lorentzian)	Field distribution width (T) (Gaussian)	Isomer shift	Area ratio A (%)
Fe standard	0	...	α -Fe (Fe)	33	0.134 ± 0.002	...	0	100
FeAl	0	3.84	α -Fe (FeAl)	32.81 ± 0.02	0.143 ± 0.004	...	0	100
FeAlN	4.6	4	α -Fe+N	32.97 ± 0.01	0.141 ± 0.002	...	0	100
FeAlN	23.9	4	γ' -Fe ₄ N (corner Fe)	34.00 ± 0.05	0.292 ± 0.011	...	0.031 ± 0.006	54.6
			γ' -Fe ₄ N (face center), ϵ -Fe ₃ N	22.99 ± 0.16	...	3.45 ± 0.15	0.256 ± 0.012	39.6
			amorphous	9.77 ± 0.95	...	2.83 ± 1.06	0.200 ± 0.081	5.8
FeAlN	44.9	3.10	ϵ -Fe ₃ N	21.00 ± 0.06	...	2.25 ± 0.07	0.325 ± 0.006	76.1
			amorphous	9.06 ± 0.48	...	3.06 ± 0.38	0.452 ± 0.033	23.9
FeAlN	53.3	...	ζ -Fe ₂ N	0.452 ± 0.000	...
FeAlN	69.3	...	ζ -Fe ₂ N	0.434 ± 0.001	...
FeAlN	99.4	...	ζ -Fe ₂ N	0.389 ± 0.002	...
FeAlN	4.0	3.94	α -Fe+N	32.87 ± 0.01	0.171 ± 0.002	...	0	100

ϵ -Fe₃N, causing the chemical environment to change and leading to the larger isomer shift and linewidth (Lorentzian or Gaussian). The ratio of the two Fe sites in pure γ' -Fe₄N were reported to be 3 (face center Fe) to 1 (corner Fe). The ratio of these two components in the FeAlN sample with N/Fe=23.9% does not agree with this value, indicating that the phase transformation is not complete. XRD spectra of this sample did not show clear phases, supporting the results from CEMS analysis.

With further N doping in the FeAlN sample with N/Fe=44.9%, a clear peak appears as shown in Fig. 2 and is identified as ϵ -Fe₃N both from the peak position in the XRD spectrum as shown in Fig. 1 and from $B_{\text{hf}} \approx 21$ T as shown in Table I.⁴ A small amount of amorphous Fe-N exists in this film from CEMS spectra as shown in Table I.

In the FeAlN films with N/Fe=53.3%, 69.3% and 99.4%, the N doping is much heavier. A clear peak in the XRD spectrum is identified as the signature of ζ -Fe₂N. ζ -Fe₂N is nonmagnetic, leading the disappearance of the local magnetic field that generates the splitting of the energy level and therefore the degeneration of the sextet of CEMS spectrum as shown in Fig. 2. There is an obvious shift of the peak from the center, indicating a large isomer shift caused by the N-induced local chemical environment. These nonmagnetic spectra were fitted with quadrupole doublets. It is noted that an XRD peak appears in FeAlN samples with N/Fe=69.3% and 99.4% at $2\theta \approx 34^\circ$, indicating the presence of Si₃N₄, which was generated by the interaction between the excess N and Si substrates.

From the hysteresis loops reported previously,² FeAl and Fe films had isotropic loops. Mildly doped FeAlN films (N/Fe=4.6% and 4.0%) had well-defined UMA. Heavy N doping lead to weak or isotropic loops. CEMS and XRD data of the FeAlN sample with N/Fe=4.6% indicate that the doped

N atoms occupy the interstitial sites in the Fe local environment. It is suggested that a preferential N distribution could generate a lattice strain field in a preferred direction defined by the bias field during deposition and therefore give rise to the observed UMA.

It is shown in Table I that B_{hf} in the corresponding Fe-N components are mostly much smaller than 33 T of the α -Fe, giving rise to the reduction of the film saturation magnetization (M_s) and the related properties such as permeability and anisotropy constant. The corner Fe in γ' -Fe₄N has $B_{\text{hf}} \approx 34$ T but only a portion of the FeAlN film with N/Fe=23.9% is in this state. The lower $B_{\text{hf}} \approx 23$ T of the face center Fe site in γ' -Fe₄N, $B_{\text{hf}} \approx 21$ T of the Fe site in ϵ -Fe₃N, the nonmagnetic ζ -Fe₂N, and the small amount of amorphous Fe-N state all contribute to the dilution of M_s at heavy N doping.

By tilting the FeAlN sample with N/Fe=4.6% at 54.7° to the incidence direction of the unpolarized γ -ray beam during the CEMS measurements, no significant differences were observed when the γ -ray beam was aligned along the magnetic easy axis and hard axis, respectively. It was shown⁶ that using an unpolarized γ -ray beam, the only information that could be extracted from this type of orientation measurement is the peak intensity ratio (R) of the peaks 2 and 5 over peaks 3 and 4 in the sextet, which gives the magnetic texture of the film (how the spins are distributed), but not the directional differences of the local structural properties.

¹K. M. Minor and J. A. Barnard, J. Appl. Phys. **85**, 4565 (1999).

²Y.-K. Liu and M. H. Kryder, Appl. Phys. Lett. **77**, 426 (2000).

³L. Néel, J. Phys. Radium **13**, 249 (1952).

⁴J.-F. Bobo, H. Chatbi, M. Vergnat, L. Hennet, O. Lenoble, Ph. Bauer, and M. Peicuch, J. Appl. Phys. **77**, 5309 (1995).

⁵J. Q. Xiao and C. L. Chien, Appl. Phys. Lett. **64**, 384 (1994).

⁶J. M. Greneche and F. Varret, J. Phys. C **15**, 5333 (1982).